

Estimation of evapotranspiration by FAO Penman-Monteith Temperature and Hargreaves-Samani models under temporal and spatial criteria. A case study in Duero Basin (Spain).

5 Rubén Moratíel^{1,2}, Raquel Bravo³, Antonio Saa^{1,2}, Ana M Tarquis², Javier Almorox¹

¹Department of Plant Production, Universidad Politécnica de Madrid, Avda. Complutense s/n, Madrid
28040, Spain

²CEIGRAM, Centro de Estudios e Investigación para la Gestión de Riesgos Agrarios y
10 Medioambientales, C/Senda del Rey 13, Madrid, 28040, Spain

³Ministerio de Agricultura y Pesca, Alimentación y Medio Ambiente Paseo de la Infanta Isabel 1, Madrid,
28071, Spain

Correspondence to: Rubén Moratíel (ruben.moratíel@upm.es)

15

Abstract. Use of the Evapotranspiration based scheduling method is the most common one for irrigation programming in agriculture. There is no doubt that the estimation of the reference evapotranspiration (ET_o) is a key factor in irrigated agriculture. However, the high cost and maintenance of agrometeorological stations and high number of sensors required to estimate it creates a non-plausible situation especially in rural areas. For this reason, the estimation of ET_o using air temperature, in places where wind speed, solar radiation and air humidity data are not readily available, is particularly attractive. Daily data record of 49 stations distributed over Duero basin (Spain), for the period 2000-2018, were used for estimation of ET_o based on seven models against Penman-Monteith FAO 56 with temporal (annual or seasonal) and spatial perspective. Two Hargreaves-Samani models (HS), with and without calibration, and five Penman-Monteith temperature models (PMT) were used in this study. The results show that the models' performance changes considerably depending on whether the scale is annual or seasonal. The performance of the seven models was acceptable at an annual perspective ($R^2 > 0.91$, $NSE > 0.88$, $MAE < 0.52 \text{ mm} \cdot \text{d}^{-1}$ and $RMSE < 0.69 \text{ mm} \cdot \text{d}^{-1}$). For winter, no model showed a good performance. In the rest of the seasons, the models with the best performance were three: PMT_{CUH} [Penman-Monteith temperature with calibration of Hargreaves empirical coefficient (k_{RS}), average monthly value of wind speed and average monthly value of maximum and minimum relative humidity], HS_C [Hargreaves-Samani with calibration of k_{RS}] and PMT_{OUH} [Penman-Monteith temperature without calibration of k_{RS} , average monthly value of wind speed and average monthly value of maximum and minimum relative humidity]. HS_C model presents a calibration of Hargreaves empirical coefficient (k_{RS}). In PMT_{CUH} model, k_{RS} was calibrated and average monthly values were used for wind speed, maximum and minimum relative humidity. Finally, PMT_{OUH} model is as PMT_{CUH} model except that k_{RS} was not calibrated. These results

35

are very useful to adopt appropriate measures for an efficient water management, especially in the intensive agriculture in semi-arid zones, under the limitation of agrometeorological data.

40

1. Introduction

A growing population and its demand for food increasingly demand natural resources such as water. This, linked with the uncertainty of climate change, makes water management a key point for future food security. The main challenge is to produce enough food for a growing population that is directly affected by the challenges set in the management of agricultural water, mainly with irrigation management (Pereira, 2017).

Evapotranspiration (ET) is the water lost from the soil surface and surface leaves by evaporation and, by transpiration, from vegetation. ET is one of the major components of the hydrologic cycle and represented a loss of water from the drainage basin. Evapotranspiration (ET) information is key to understanding and managing water resources systems (Allen et al., 2011). ET is normally modeled using weather data and algorithms that describe aerodynamic characteristics of the vegetation and surface energy.

In agriculture, irrigation water is usually applied based on the water balance method in the soil water balance equation that allows the calculation of the decrease in soil water content as the difference between outputs and inputs of water to the field. In arid areas where rainfall is negligible during the irrigation season an average irrigation calendar may be defined a priori using mean ET values (Villalobos et al., 2016). The Food and Agricultural Organization of United Nations (FAO) improved and upgraded the methodologies for reference evapotranspiration (ET_o) estimation by introducing the reference crop (grass) concept, described by FAO Penman- Monteith (PM- ET_o) equation (Allen et al., 1998). This approach was tested well under different climates and time step calculations and is currently adopted worldwide (Allen et al., 1998, Todorovic et al., 2013; Almorox et al., 2015). To estimate crop evapotranspiration (ET_c) is obtained by function of two factor ($ET_c = K_c \cdot ET_o$): reference crop evapotranspiration (ET_o) and crop coefficient (K_c) (Allen et al. 1998). ET_o was introduced to study the evaporative demand of the atmosphere independently of crop type, crop stage development and management practices. ET_o is only affected by climatic parameters, and is computed from weather data. Crop influences are accounted for by using a specific crop coefficient (K_c). However, K_c varies predominately with the specific crop characteristics and only to a limited extent with climate (Allen et al., 1998)

The ET is very variable locally and temporarily because of the climate differences. Because the ET component is relatively large in water hydrology balances any small error in its estimate or measurement represents large volumes of water (Allen et al., 2011). Small deviations in ET_o estimations would affect irrigation and water management in rural areas in which crop extension is significant. For example, in 2017 there was a water shortage at the beginning of the cultivation period (March) at the Duero basin (Spain). The classical irrigated crops, i.e. corn, were replaced by others with lower water needs such as sunflower.

Wind speed (u), solar radiation (R_s), relative humidity (RH) and temperature (T) of the air are required to estimate ET_o . Additionally, vapor pressure deficit (VPD), soil heat flux (G) and net radiation (R_n) measurements or estimates are necessary. The PM- ET_o methodology presents the disadvantage that
80 required climate or weather data that are normally unavailable or low quality (Martinez and Thepadia, 2010) in rural areas. In this case, where data are missing, Allen et al. (1998) in the guidelines for PM- ET_o recommend two approaches: a) using equation of Hargreaves-Samani (Hargreaves and Samani, 1985) and b) using PM temperature (PMT) method that requires data of temperature to estimate R_n (net radiation) and VPD for obtaining ET_o . In these situations, temperature-based evapotranspiration (TET) methods are
85 very useful (Mendicino and Senatore, 2012). Air temperature is the most available meteorological data, which are readily from most of climatic weather station. Therefore, TET methods and temperature databases are solid base for ET estimation all over the world including areas with limited data resources (Droogers and Allen, 2002). The first reference of the use of PMT for limited meteorological data was Allen (1995), subsequently, studies like those of Allen et al. (1996), Annandale et al. (2002), were carried
90 out with similar behavior to HS and FAO-PM, although there was the disadvantage of a greater preparation and computation of the data than the HS method. On this point, it should be noticed that the researchers do not favor to using PMT formulation and adopting the HS equation, simpler and easier to use (Paredes et al., 2018). Authors like Pandey et al. (2014) performed calibrations based on solar radiations coefficients in Hargreaves-Samani equations. Today, PMT calculation process is easily
95 implemented with the new computers (Pandey and Pandey, 2016; Quej et al., 2019). Todorovic et al., (2013) reported that, in Mediterranean hyper-arid and arid climates PMT and HS show a similar behavior and performance while for moist sub-humid areas the best performance was obtained by PMT method. This behavior was reported for moist sub-humid areas in Serbia (Trajovic, 2005). Several studies confirm this performance in a range of climates (Martinez and Thepadia, 2010; Raziei and Pereira,
100 2013; Almorox, et al., 2015; Ren et al., 2016). Both models (HS and PMT) improved when local calibrations are performed (Gavilán et al., 2006; Paredes et al., 2018). These reduce the problem when wind speed and solar radiation are the major driving variables.

Studies in Spain comparing HS and PMT methodologies were studied in moist sub-humid climate zones (Northern Spain) showing a better fit in PMT than in HS. (Lopez Moreno et al., 2009). Tomas-Burguera
105 (2017) reported for the Iberian Peninsula a better adjustment of PMT than HS, provided that the lost values were filled by interpolation and not by estimation in the model of PMT.

Normally the calibration of models for ET_o estimation is done from a spatial approach, calibrating models in the locations studied. Very few studies have been carried out to test models from the seasonal point of view, being the annual calibration being the most studied. Meanwhile spatial and annual approaches are
110 of great interest for climatology and meteorology, for agriculture, seasonal or even monthly calibrations are relevant for crop (Nouri and Homae, 2018). To improve accuracy of ET_o estimations, Paredes et al., 2018 used the values of the calibration constants values in the models were derived for October-March and April-September semesters.

The aim of this study was to evaluate the performance of temperature models for the estimation of
115 reference evapotranspiration against the FAO56 Penman Monteith, with a temporal (annual or seasonal)

and spatial perspective in the Duero basin (Spain). The models evaluated were two Hargreaves-Samani (HS), with calibration and without calibration and five Penman-Monteith temperature model (PMT) analyzing the contribution of wind speed, humidity and solar radiation in a situation of limited agrometeorological data.

120

2. Materials and Method

2.1 Description of the Study Area

The study focuses on the Spanish part of the Duero hydrographic basin. The international hydrographic Duero basin is the most extensive of the Iberian Peninsula with 98073 km², it includes the territory of the Duero river basin as well as the transitional waters of the Oporto Estuary and the associated Atlantic coastal ones (CHD, 2019). It is a shared territory between Portugal with 19214 km² (19.6 % of the total area) and Spain with 78859 km² (80.4%). The Duero river basin is located in Spain between the parallels 43° 5' N and 40° 10' N and the meridians 7° 4' W and 1° 50' W (Fig. 1). This basin is almost exactly with the so-called *Submeseta Norte*, an area with an average altitude of 700 m, delimited by mountain ranges with a much drier central zone that contains large aquifers, being the most important area of agricultural production. The Duero Basin belongs in its 98.4% to the Autonomous Community of *Castilla y León*. The 70% of the average annual precipitation is used directly by the vegetation or evaporated from surface, this represents 35.000 hm³. The remaining (30%) is the total natural runoff. Mediterranean is the predominant climate. The 90% of surface is affected by summer drought conditions. The average annual values are: 12 °C of temperature and 612 mm of precipitation. However, precipitation ranges from minimum values of 400 mm (South-Central area of the basin) to a maximum of 1800 mm in the northeast of the basin (CHD, 2019). According to Lautensach (1967), 30 mm is the threshold definition of a dry month. Therefore, between 2 and 5 dry periods can be found in the basin (Ceballos et al., 2004). Moreover, the climate variability, especially precipitation, exhibited in the last decade has decreased the water availability for irrigation in this basin (Segovia- Cardozo et al., 2019).

The Duero basin has 4 million hectares of rainfed crops and some 500,000 hectares irrigated that consumes 75% of the basin's water resources consumption. Barley (*Hordeum vulgare* L.) is the most important rainfed crop in the basin occupying 36% of the National Crop Surface followed by wheat (*Triticum aestivum* L.) with 30% (MAPAMA, 2019). Sunflower (*Helianthus annuus* L.) representing 30% of the National crop surface. This crop is mainly unirrigated (90%). Maize (*Zea mays* L.), alfalfa (*Medicago sativa* L.) and sugar beet (*Beta vulgaris* L. var. *sacharifera*) are the main irrigated crops. These crops representing 29 %, 30% and 68% of each National crop area, respectively. Finally, Vine (*Vitis vinifera* L.) fills 72000 ha being less than 10% irrigated. For the irrigated crops of the basin there are water allocations that fluctuate depending on the availability of water during the agricultural year and the type of crop. These values fluctuate from 1200-1400 m³ / ha for vine up to 6400-7000 m³/ha for maize and alfalfa. The use rates of the irrigation systems used in the basin are: 25 %, 68% and 7% for surface, sprinkler and drip irrigation respectively (*Plan Hidrológico*, 2019).

150

155

160

165

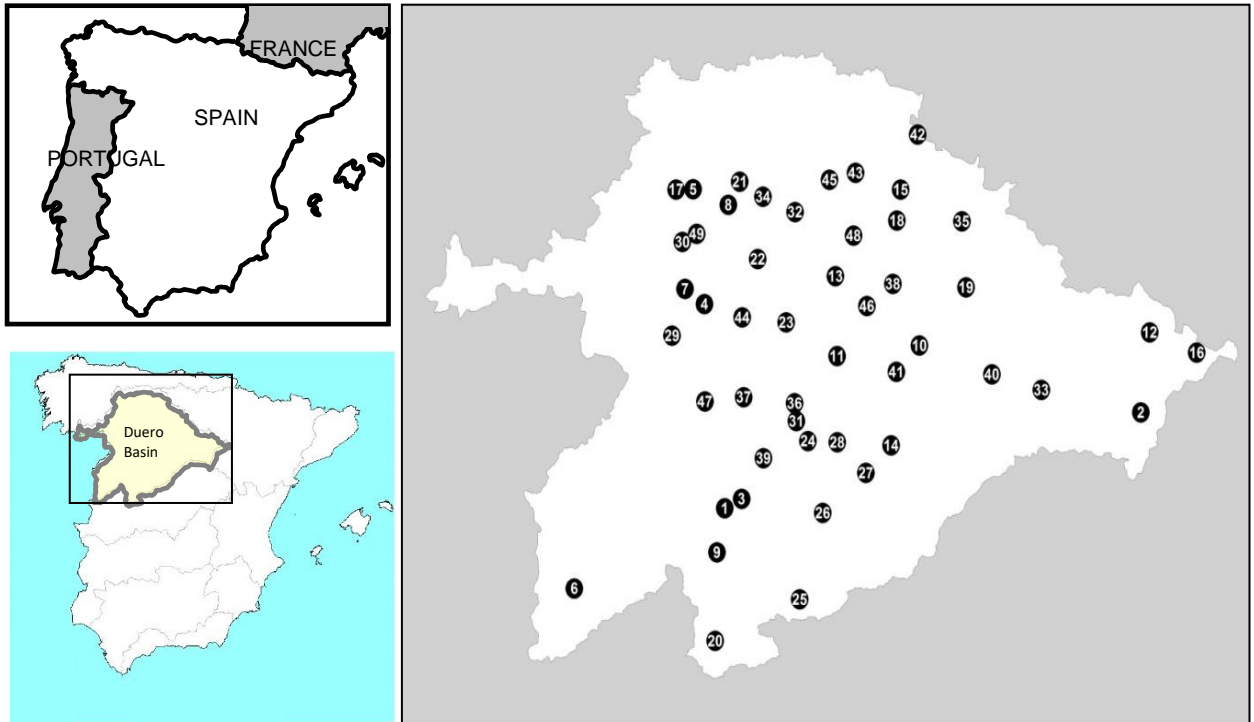


Figure. 1. Location of study area. The point with the number indicates the location of the agrometeorological stations according to Table 1.

170

2.2 Meteorological Data

175

180

185

The daily climate data were downloaded from 49 stations (Fig. 1B) from the agrometeorological network SIAR (Irrigation Agroclimatic Information System; SIAR in Spanish language), which is managed by the Spanish Ministry of Agriculture, Food and Environment (SIAR, 2018). The SIAR is coordinated by the Ministry of Agriculture, Fisheries and Food providing the basic meteorological data from weather stations distributed throughout the Duero Basin (Table 1). Each station incorporates measurements of air temperature (T) and relative humidity (RH; Vaisala HMP155), precipitation (ARG100 rain gauge), solar global radiation (pyranometer SKYE SP1110) and wind direction and wind speed (u) (wind vane and RM YOUNG 05103 anemometer). Sensors were periodically maintained and calibrated, and all data were recorded and averaged hourly on a data logger (Campbell CR10X and CR1000). Characteristics of the agrometeorological stations were described by (Moratiel et al., 2011, 2013a). For quality control, all parameters were checked, the sensors were periodically maintained and calibrated, all data being recorded and hourly averaged on a data logger. The database calibration and maintenance are carried out by the Ministry of Agriculture. Transfer of data from stations to the Main Center is accomplished by modems; the Main Center incorporates a server, which sequentially connects to each station to download the information collected during the day. Once the data from the stations are downloaded, they are processed and transferred to a database. The Main Center is responsible for quality control procedures that comprise

the routine maintenance program of the network, including sensor calibration, checked for validity values and data validation. Moreover, the database was analyzed to find incorrect or missing values. To ensure that good quality data were used, we used quality control procedures to identify erroneous and suspect data. The quality control procedures applied are the range/limit test, step test consistency and an internal test (Estevez et al., 2016).

The period studied was from 2000 to 2018, although the start date may fluctuate depending on the availability of data. Table 1 shows the coordinates of the agrometeorological stations used in the Duero Basin and the aridity index based on UNEP (1997). Table 1 the predominance of the semi-arid climate zone with 42 stations of the 49, being 2 arid, 4 dry-sub humid and 1 moist sub-humid.

Table 1. Agrometeorological station used in the study. Coordinates and Aridity Index.

Stations	Latitude ⁽¹⁾	Longitude ⁽¹⁾	Altitude (m)	Aridity Index
1 Aldearrubia	40.99	-5.48	815	moist sub-humid
2 Almazán	41.46	-2.50	943	semi-arid
3 Arabayona	41.04	-5.36	847	semi-arid
4 Barcial del Barco	41.93	-5.67	738	semi-arid
5 Bustillo del Páramo	42.46	-5.77	874	semi-arid
6 Ciudad Rodrigo	40.59	-6.54	635	semi-arid
7 Colinas de Trasmonte	42.00	-5.81	709	semi-arid
8 Cubillas de los Oteros	42.40	-5.51	769	semi-arid
9 Ejeme	40.78	-5.53	816	semi-arid
10 Encinas de Esgueva	41.77	-4.10	816	semi-arid
11 Finca Zamadueñas	41.71	-4.70	714	semi-arid
12 Fuentecantos	41.83	-2.43	1063	semi-arid
13 Fuentes de Nava	42.08	-4.72	744	semi-arid
14 Gomezserracín	41.30	-4.30	870	semi-arid
15 Herrera de Pisuerga	42.49	-4.25	821	semi-arid
16 Hinojosa del Campo	41.73	-2.10	1043	semi-arid
17 Hospital de Orbigo	42.46	-5.90	835	semi-arid
18 Lantadilla	42.34	-4.28	798	semi-arid
19 Lerma	42.04	-3.77	840	semi-arid
20 Losar del Barco	40.37	-5.53	1024	semi-arid
21 Mansilla mayor	42.51	-5.43	791	semi-arid
22 Mayorga	42.15	-5.29	748	semi-arid
23 Medina de Rioseco	41.86	-5.07	739	semi-arid
24 Medina del Campo	41.31	-4.90	726	arid
25 Muñozgalindo	40.58	-4.93	1128	arid
26 Nava de Arévalo	40.98	-4.78	921	semi-arid
27 Nava de la Asunción	41.17	-4.48	822	semi-arid
28 Olmedo	41.31	-4.69	750	semi-arid
29 Pozuelo de Tábara	41.78	-5.90	714	semi-arid
30 Quintana del Marco	42.22	-5.84	750	semi-arid

31	Rueda	41.40	-4.98	709	semi-arid
32	Sahagún	42.37	-5.02	856	semi-arid
33	San Esteban de Gormaz	41.56	-3.22	855	semi-arid
34	Santas Martas	42.44	-5.26	885	semi-arid
35	Tardajos	42.35	-3.80	770	dry sub-humid
36	Tordesillas	41.49	-5.00	658	semi-arid
37	Toro	41.51	-5.37	650	semi-arid
38	Torquemada	42.05	-4.30	868	semi-arid
39	Torrecilla de la Orden	41.23	-5.21	793	semi-arid
40	Vadocondes	41.64	-3.58	870	semi-arid
41	Valbuena de Duero	41.64	-4.27	756	semi-arid
42	Valle de Valdelucio	42.75	-4.13	975	dry sub-humid
43	Villaeles de Valdavia	42.56	-4.59	885	semi-arid
44	Villalpando	41.88	-5.39	701	semi-arid
45	Villaluenga de la Vega	42.53	-4.77	927	dry sub-humid
46	Villamuriel de Cerrato	41.95	-4.49	750	dry sub-humid
47	Villaralbo	41.48	-5.64	659	semi-arid
48	Villoldo	42.27	-4.59	817	semi-arid
49	Zotes del Páramo	42.26	-5.74	779	semi-arid

⁽¹⁾ Degrees

2.3 Estimates of Reference Evapotranspiration

2.3.1 FAO Penman-Monteith (FAO-PM)

205 The FAO recommend the PM method as the one for computing ET_o and evaluating other ET_o models
like the Penman-Monteith model using only temperature data (PMT) and other temperature-based model
(Allen et al., 1998). The method estimates the potential evapotranspiration from a hypothetical crop with
an assumed height of 0.12 m having aerodynamic resistance of $(r_a) 208/u_2$, (u_2 is the mean daily wind
speed measured at a 2 m height over the grass) and a surface resistance (r_s) of $70 \text{ s}\cdot\text{m}^{-1}$ and an albedo of
210 0.23, closely resembling the evaporation of an extension surface of green grass of uniform height,
actively growing and adequately watered. The ET_o ($\text{mm}\cdot\text{d}^{-1}$) was estimated following FAO-56 (Allen et
al. 1998):

$$ET_o = \frac{0.408 \Delta (R_n - G) + \gamma \frac{900}{T + 273} u_2 (e_s - e_a)}{\Delta + \gamma(1 + 0.34u_2)} \quad [1]$$

215 In Eq. 1, R_n is net radiation at the surface ($\text{MJ m}^{-2} \text{d}^{-1}$), G is ground heat flux density ($\text{MJ m}^{-2} \text{d}^{-1}$), γ is the
psychrometric constant ($\text{kPa } ^\circ\text{C}^{-1}$), T is mean daily air temperature at 2 m height ($^\circ\text{C}$), u_2 is wind speed at
2 m height (m s^{-1}), e_s is the saturation vapor pressure (kPa), e_a is the actual vapor pressure (kPa) and Δ is
the slope of the saturation vapor pressure curve ($\text{kPa } ^\circ\text{C}^{-1}$). According to Allen et al. (1998) in Eq. 1, G
can be considered as zero.

220 2.3.2 Hargreaves-Samani (HS)

The scarce availability of agrometeorological data (global solar radiation, air humidity and wind speed mainly) limit the use of the FAO-PM method in many locations. Allen et al., (1998) recommended applying Hargreaves–Samani expression for situations where only the air temperature is available. The Hargreaves-Samani formulation (HS) is an empirical method that requires empirical coefficients to calibrate (Hargreaves and Samani, 1982, 1985). The Hargreaves and Samani (Hargreaves and Samani, 1982, 1985) method is given by the following equation (2):

$$ET_o = 0.0135 \cdot k_{RS} \cdot 0.408 \cdot H_o \cdot (T_m + 17.8) \cdot (T_x - T_n)^{0.5} \quad (2)$$

where ET_o is the reference evapotranspiration (mm day^{-1}); H_o is extraterrestrial radiation ($\text{MJ}\cdot\text{m}^{-2}\cdot\text{d}^{-1}$); k_{RS} is the Hargreaves empirical coefficient, T_m , T_x and T_n are the daily mean, maximum and minimum air temperature ($^{\circ}\text{C}$), respectively. The value k_{RS} was initially set to 0.17 for arid and semiarid regions (Hargreaves and Samani, 1985). Hargreaves (1994) later recommended to use the value of 0.16 for interior regions and 0.19 for coastal regions. Daily temperature variations can occur due to other factors such as topography, vegetation, humidity, among others, thus using a fixed coefficient may lead to errors. In this study, we use the 0.17 as original coefficient (HS_o) and the calibrated coefficient k_{RS} (HS_c). The k_{RS} reduces the inaccuracy and consequently thus improving the estimation of ET_o . This calibration was done for each station.

2.3.3 Penman- Monteith Temperature (PMT)

The FAO-PM, when applied using only measured temperature data is denominated to as Penman-Monteith Temperature (PMT) retains many of the dynamics of the full data FAO-PM (Pereira et al., 2015; Hargreaves and Allen, 2003). Humidity and solar radiation are estimated in the PMT model using only air temperature as input for the calculation of ET_o . Wind speed in the PMT model is set as constant value of 2m/s (Allen et al.1998). In this model, where global solar radiation (or sunshine data) is lacking, the difference between the maximum and minimum temperature can be used, as an indicator of cloudiness and atmospheric transmittance, for the estimation of solar radiation [Eq.3] (Hargreaves and Samani, 1982). Net solar shortwave and longwave radiation estimates are obtained as indicated by Allen et al., (1998), equation 4 and 5 respectively. The expression of PMT is obtained as indicated in equations 4, 5, 6, 7 and 8.

$$R_s = H_o \cdot k_{RS} \cdot (T_x - T_n)^{0.5} \quad (3)$$

$$R_{ns} = 0.77 \cdot H_o \cdot k_{RS} \cdot (T_x - T_n)^{0.5} \quad (4)$$

where R_s is solar radiation ($\text{MJ}\cdot\text{m}^{-2}\cdot\text{d}^{-1}$) ; R_{ns} is net solar shortwave radiation ($\text{MJ}\cdot\text{m}^{-2}\cdot\text{d}^{-1}$); H_o is extraterrestrial radiation ($\text{MJ}\cdot\text{m}^{-2}\cdot\text{d}^{-1}$); H_o was computed as a function of site latitude, and solar angle and the day of the year (Allen et al., 1998). T_x is daily maximum air temperature ($^{\circ}\text{C}$), T_n is daily minimum air temperature ($^{\circ}\text{C}$). For k_{RS} Hargreaves (1994) recommended to use $k_{RS} = 0.16$ for interior regions and $k_{RS} = 0.19$ for coastal regions. For better accuracy the coefficient k_{RS} can be adjusted locally (Hargreaves

and Allen 2003). In this study two assumptions of k_{RS} were made, one where a value of 0.17 was fixed and another where it was calibrated for each station.

$$R_{nl} = \left(1.35 \cdot \left(\frac{k_{RS} \cdot (T_x - T_n)^{0.5}}{0.75 - 2 \times 10^{-5}} \right) - 0.35 \right) \cdot \left(0.34 - 0.14 \left(0.6108 \cdot \exp \left(\frac{17.27 \cdot T_d}{T_d - 237.3} \right) \right)^{0.5} \right) \cdot \sigma \cdot \left(\frac{(T_x + 273.15)^4 + (T_n + 273.15)^4}{2} \right) \quad (5)$$

260

Where R_{nl} is net longwave radiation ($\text{MJ} \cdot \text{m}^{-2} \cdot \text{d}^{-1}$) T_x is daily maximum air temperature ($^{\circ}\text{C}$); T_n is daily minimum air temperature ($^{\circ}\text{C}$); T_d is dew point temperature ($^{\circ}\text{C}$) calculated with the T_n according to Todorovic et al., 2013; σ Stefan-Boltzmann constant for a day ($4.903 \cdot 10^{-9} \text{ MJ K}^{-4} \text{ m}^{-2} \text{ d}^{-1}$); z is the altitude (m).

265

$$PMT_{rad} = \left(\frac{0.408 \Delta}{\Delta + \gamma(1 + 0.34u_2)} \right) \cdot (R_{ns} - R_{nl} - G) \quad (6)$$

$$PMT_{aero} = \frac{\gamma \cdot \frac{900 \cdot u_2}{T_m + 273} \cdot \left(\frac{e_s(T_x) + e_s(T_n)}{2} \right) - e_s(T_d)}{\Delta + \gamma(1 + 0.34u_2)} \quad (7)$$

$$PMT = PMT_{rad} + PMT_{aero} \quad (8)$$

270

Where PMT is the reference evapotranspiration estimate by Penman-Monteith temperature method ($\text{mm} \cdot \text{d}^{-1}$); PMT_{rad} is the radiative component of PMT ($\text{mm} \cdot \text{d}^{-1}$); PMT_{aero} is the aerodynamic component of PMT ($\text{mm} \cdot \text{d}^{-1}$); Δ is the slope of the saturation vapor pressure curve ($\text{kPa } ^{\circ}\text{C}^{-1}$), γ is the psychrometric constant ($\text{kPa } ^{\circ}\text{C}^{-1}$), R_{ns} is net solar shortwave radiation ($\text{MJ m}^{-2} \cdot \text{d}^{-1}$), R_{nl} is net longwave radiation ($\text{MJ m}^{-2} \cdot \text{d}^{-1}$), G is ground heat flux density ($\text{MJ m}^{-2} \text{ d}^{-1}$) considered zero according to Allen et al.1998, T_m is mean daily air temperature ($^{\circ}\text{C}$), T_x is maximum daily air temperature, T_n is mean daily air temperature, T_d is dew point temperature ($^{\circ}\text{C}$) calculated with the T_n according to Todorovic et al. (2013), u_2 is wind speed at 2 m height (m s^{-1}) and e_s is the saturation vapor pressure (kPa). In this model two assumptions of k_{RS} were done, one where a value of 0.17 was fixed and another where it was calibrated for each station.

280

2.3.4 Calibration and models

We studied two methods to estimate the ETo: Hargreaves–Samani (HS) and reference evapotranspiration estimate by Penman-Monteith temperature (PMT). Within these methods, different adjustments are proposed based on the adjustment coefficients of the methods and the missing data. The parametric calibration for the 49 stations was applied in this study. In order to decrease the errors of the evapotranspiration estimates, local calibration was used. The seven methods used with the coefficient

285

(k_{RS}) of the calibrated and characteristics in the different locations studied are showed in Table 2. The calibration of the model coefficients was achieved by the nonlinear least squares fitting technique. The analyzed were calculated on yearly and seasonal bases. The seasons were the following: (1) winter (December, January, and February or DJF), (2) spring (March, April, and May or MAM), (3) summer (June, July, and August or JJA), (4) autumn (September, October, and November or SON).

Table 2. Characteristics of the models used in this study.

Model	Coefficient k_{RS}	u_2 (m/s)	Td (°C)
HS _O	0.17	-	-
HS _C	Calibrated	-	-
PMT _{O2T}	0.17	2	Todorovic ⁽¹⁾
PMT _{C2T}	Calibrated	2	Todorovic ⁽¹⁾
PMT _{OUT}	0.17	Average ⁽²⁾	Todorovic ⁽¹⁾
PMT _{OUH}	0.17	Average ⁽²⁾	Average ⁽³⁾
PMT _{CUH}	Calibrated	Average ⁽²⁾	Average ⁽³⁾

⁽¹⁾Dew point temperature obtained according to Todorovic et al. (2013).

⁽²⁾Average monthly value of wind speed

⁽³⁾Average monthly value of maximum and minimum relative humidity.

2.4. Performance assessment.

Model's suitability, accuracy and performance were evaluated using coefficient of determination (R^2 ; Eq. [9]) of the n pairs of observed (O_i) and predicted (P_i) values. Also, the mean absolute error (MAE, $mm \cdot d^{-1}$; Eq. [10]), root mean square error (RMSE; Eq. [11]) and The Nash-Sutcliffe model efficiency coefficient (NSE; Eq. [12]) (Nash and Sutcliffe 1970) was used. The coefficient of regression line (b), forced through the origin, is obtained by predicted values divided by observed values (ET_{model}/ET_{FAO56}). The results were represented in a map applying of the Kriging method with the Surfer® 8 program.

$$R^2 = \left\{ \frac{\sum_{i=1}^n (O_i - \bar{O}) \cdot (P_i - \bar{P})}{[\sum_{i=1}^n (O_i - \bar{O})^2]^{0.5} \cdot [\sum_{i=1}^n (P_i - \bar{P})^2]^{0.5}} \right\}^2 \quad (9)$$

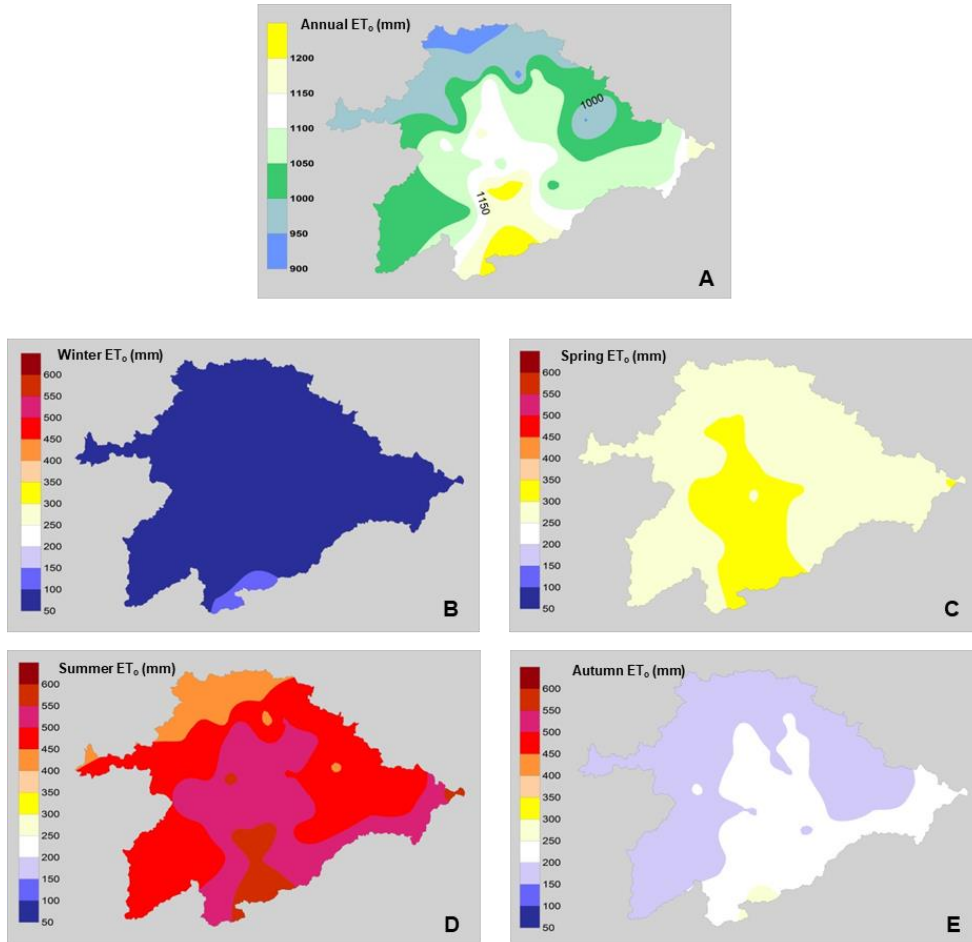
$$MAE = \frac{1}{n} \sum_{i=1}^n (|O_i - P_i|) \quad (mm \cdot d^{-1}) \quad (10)$$

$$RMSE = \left[\frac{\sum_{i=1}^n (O_i - P_i)^2}{n} \right]^{0.5} \quad (mm \cdot d^{-1}) \quad (11)$$

$$NSE = 1 - \left[\frac{\sum_{i=1}^n (O_i - P_i)^2}{\sum_{i=1}^n (O_i - \bar{O})^2} \right] \quad (12)$$

310 **3. Results and Discussion**

In the study period the data indicated that the Duero basin is characterized by being a semiarid climate zone (94% of the stations) where the P / ET_o ratio is between 0.2-0.5 (Todorovic et al., 2013). The mean annual rainfall is 428 mm while the average annual ET_o for Duero basin is of 1079 mm, reaching the maximum values in the zone center-south with values that surpass slightly 1200 mm (Fig. 2). The great temporal heterogeneity is observed in the Duero Basin with values of 7% of the ET_o during the winter months (DJF) while during the summer months (JJA) they represent 47% of the annual ET_o . In addition, the months from May till September represent 68% of the annual ET_o , with similar values as reported by Moratiel et al. (2011).



320 Figure.2. Mean values season of ET_o (mm) during the study period 2000-2018. A, annual; B, winter (December, January, and February or DJF); C, spring (March, April, and May or MAM); D, summer (June, July, and August or JJA) and E, autumn (September, October, and November or SON).

325 Table 3 shows the different statistics analyzed in the seven models studied as a function of the season of the year and annually. From an annual point of view all the models show R^2 values higher than 0.91, NSE higher than 0.88, MAE less than 0.52, RMSE lower than 0.69 and underestimates or overestimates of the models by $\pm 4\%$. The best behaviour is shown by the PMT_{CHU} model with MAE and RMSE of $0.39 \text{ mm}\cdot\text{d}^{-1}$ and $0.52 \text{ mm}\cdot\text{d}^{-1}$ respectively. PMT_{CHU} shows no tendency to overestimate or underestimate the values

330 in which it is observed a coefficient of regression b of 1.0. This model show values of NSE and R^2 of
 0.93. The models HSc and PMT_{OUH} have a similar behavior with same MAE ($0.41 \text{ mm}\cdot\text{d}^{-1}$), NSE (0.92)
 and R^2 (0.91). RMSE is $0.55 \text{ mm}\cdot\text{d}^{-1}$ for PMT_{OUH} model and $0.54 \text{ mm}\cdot\text{d}^{-1}$ for HSc model. The models
 PMT_{OUT} and HSo showed a slightly higher performance than PMT_{O2T} and PMT_{C2T} , being these last two
 335 PMT_{OUH}] improve as the averages of wind speed (u) and dew temperature (T_d) values are incorporated.
 The same pattern is shown between the PMT_{CUH} models, where the mean u values and T_d are
 incorporated, and PMT_{C2T} , with u of 2 m/s and dew temperature with the approximation of Todorovic et
 al. (2013). These adjustments are supported because the adiabatic component of evapotranspiration in the
 PMT equation is very influential in the Mediterranean climate, especially wind speed (Moratiel et al.,
 340 2010).

From a spatial perspective, it is observed in Fig. 3 that the areas where the values of MAE are higher are
 to the east and southwest of the basin. This is due to the fact that the average wind speed in the eastern
 zone is higher than 2.5 m/s, for example, the Hinojosa del Campo station shows average annual values of
 3.5 m/s. The southwest area shows values of wind speeds below 1.5 m/s as the Ciudad Rodrigo station
 345 with annual average values of 1.19 m/s.

Table 3. Statistical indicators for ET_o estimation in the seven models studied for different season. Average data for the 49 stations studied.

Season	Variable	MODEL							Daily Average (ETFAO5 6, $\text{mm}\cdot\text{d}^{-1}$)
		HSo	HSc	PMT_{O2T}	PMT_{C2T}	PMT_{OUT}	PMT_{OUH}	PMT_{CUH}	
Annual	R^2	0.93	0.93	0.91	0.91	0.92	0.93	0.93	2.95
	NSE	0.90	0.92	0.88	0.89	0.90	0.92	0.93	
	MAE ($\text{mm}\cdot\text{d}^{-1}$)	0.47	0.41	0.52	0.50	0.47	0.41	0.39	
	RMSE($\text{mm}\cdot\text{d}^{-1}$)	0.62	0.54	0.69	0.66	0.62	0.55	0.52	
	RMSE (%)	21.0	18.5	23.4	22.3	20.9	18.7	17.8	
	b	1.03	0.97	1.04	1.02	1.03	1.03	1.00	
Winter (DJF)	R^2	0.53	0.53	0.56	0.55	0.56	0.59	0.59	0.90
	NSE	0.43	0.50	0.36	0.35	0.35	0.57	0.58	
	MAE ($\text{mm}\cdot\text{d}^{-1}$)	0.27	0.25	0.29	0.30	0.30	0.24	0.24	
	RMSE($\text{mm}\cdot\text{d}^{-1}$)	0.35	0.33	0.36	0.37	0.37	0.30	0.30	
	RMSE (%)	38.3	36.1	40.3	40.5	41.2	33.6	33.5	
	b	0.99	0.93	1.07	1.06	1.09	0.96	0.96	
Spring (MAM)	R^2	0.83	0.83	0.81	0.81	0.81	0.82	0.82	3.19
	NSE	0.80	0.81	0.75	0.78	0.74	0.80	0.81	
	MAE ($\text{mm}\cdot\text{d}^{-1}$)	0.43	0.42	0.50	0.46	0.52	0.45	0.43	
	RMSE($\text{mm}\cdot\text{d}^{-1}$)	0.56	0.55	0.62	0.59	0.65	0.57	0.55	

	RMSE(%)	17.5	17.2	19.6	18.4	20.2	18.0	17.3	
	b	1.01	0.95	1.04	1.00	1.06	1.02	0.99	
<hr/>									
Summer									
(JJA)	R ²	0.59	0.59	0.53	0.53	0.56	0.60	0.60	
	NSE	0.32	0.54	0.21	0.31	0.45	0.52	0.59	
	MAE (mm·d ⁻¹)	0.68	0.56	0.72	0.68	0.62	0.57	0.53	5.48
	RMSE(mm·d ⁻¹)	0.84	0.71	0.91	0.87	0.79	0.73	0.68	
	RMSE(%)	15.4	13.0	16.6	15.8	14.4	13.3	12.3	
	b	1.04	0.98	1.03	1.00	1.00	1.03	1.00	
<hr/>									
Autumn									
(SON)	R ²	0.85	0.85	0.83	0.83	0.84	0.86	0.86	
	NSE	0.72	0.82	0.61	0.65	0.78	0.83	0.85	
	MAE (mm·d ⁻¹)	0.50	0.40	0.58	0.55	0.46	0.40	0.38	2.21
	RMSE(mm·d ⁻¹)	0.62	0.52	0.73	0.70	0.58	0.51	0.49	
	RMSE(%)	28.1	23.5	32.8	31.6	26.2	23.1	22.1	
	b	1.09	1.02	1.14	1.12	1.07	1.05	1.02	

350

These MAE differences are more pronounced in those models in which the average wind speed is not taken, such as the PMT_{C2T} and PMT_{O2T} models. Most of the basin takes values of wind speeds between 1.5 and 2.5 m/s. The lower MAE values in the northern zone of the basin are due to the lower average values of vapour pressure deficit (VPD) than the central area, with values of 0.7 kPa in the northern zone and 0.95 kPa in the central zone. Same trends in the effect of wind on the ETo estimates were detected by Nouri and Homaei (2018) where they indicated that values outside the range of 1.5-2.5 m/s in models where the default u was set at 2 m / s, increased the error of the ETo. Even models such as HS, where the influence of the wind speed values are not directly indicated outside the ranges previously mentioned, their performance is not good and some authors have proposed HS calibrations based on wind speeds in Spanish basins such as the Ebro Basin (Martinez-Cob and Tejero-Juste, 2004). In our study, the HS_c model showed good performance with MAE values similar to PMT_{CUH} and PMT_{OUH} (Fig.3). The performance of the models by season of the year changes considerably, obtaining lower adjustments with values of R² 0.53 for winter (DJF) in the models of HS_o and HS_c and for summer (JJA) in the models PMT_{O2T} and PMT_{C2T}. All models during spring and autumn show R² above 0.8. The NSE for models HS_o, PMT_{C2T}, PMT_{O2T} and PMT_{OUT} in summer and winter are at unsatisfactory values below 0.5 (Moriassi et al. 2007). The mean values (49 stations) of MAE and RMSE for the models in the winter were 0.24 -0.30 mm·d⁻¹ and 0.3-0.37 mm·d⁻¹ respectively. For spring, the ranges were between 0.42-0.52 mm·d⁻¹ for MAE and 0.55-0.65 mm·d⁻¹ for RMSE. In summer, MAE fluctuated between 0.53-0.72 mm·d⁻¹ and RMSE 0.68-0.91 mm·d⁻¹. Finally, in autumn, the values of MAE and RMSE were 0.38-0.58 and 0.49-0.70 mm·d⁻¹ respectively (Table 3).

370

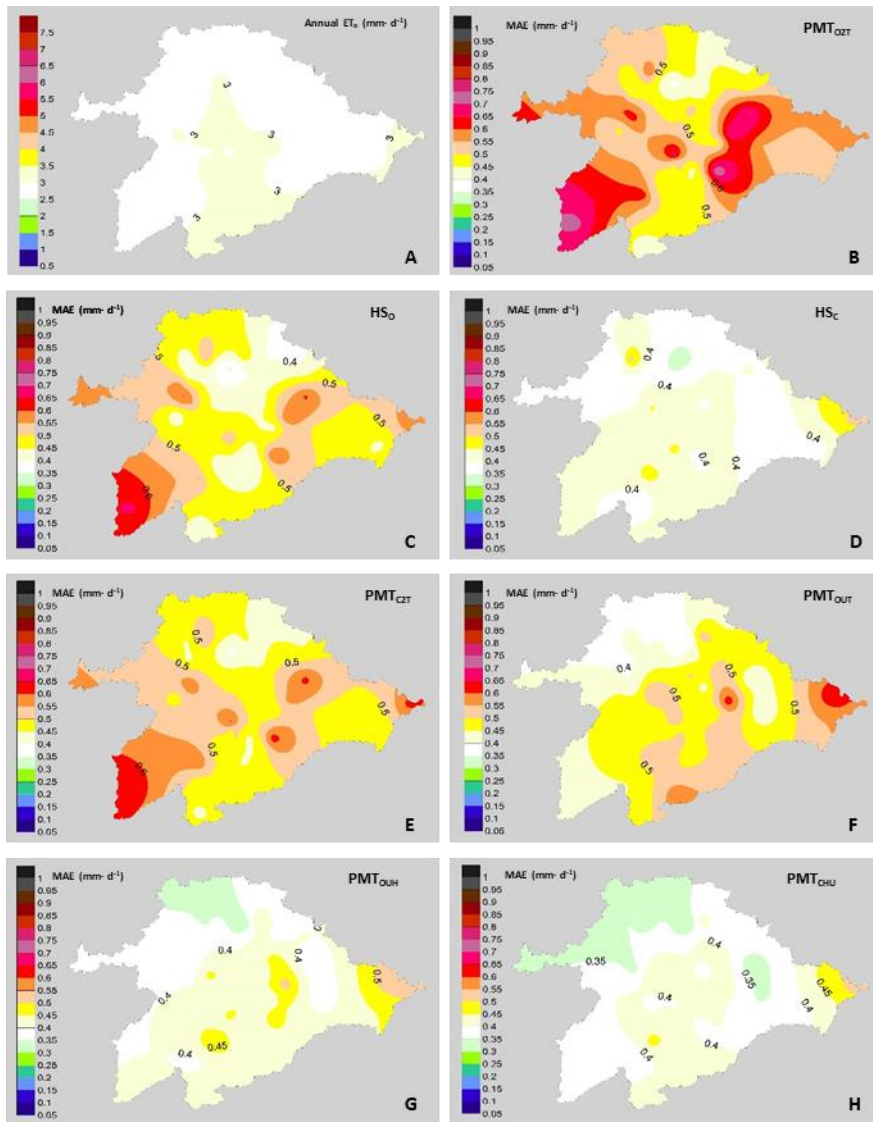


Figure 3. Performance of the models with an annual focus. A, Average annual values of ET_0 ($mm \cdot d^{-1}$). Mean values of MAE ($mm \cdot d^{-1}$): B, PMT_{O2T} model; C, H_O model; D, H_C model; E, PMT_{C2T} model; F, PMT_{OUT} model; G, PMT_{OUH} model and H, PMT_{CUH} model

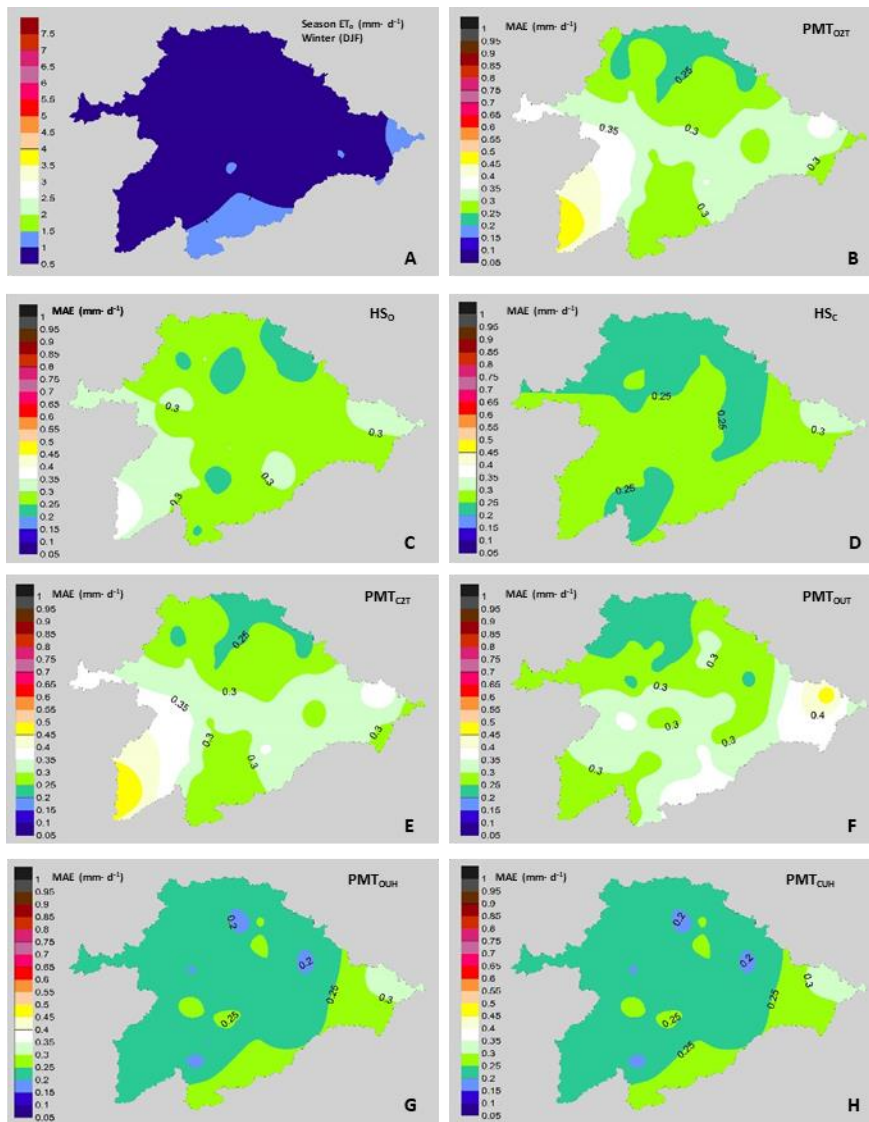


Figure 4. Performance of the models with a winter focus (December, January and February). A, Average values of ET_0 ($mm \cdot d^{-1}$) in winter. Mean values of MAE ($mm \cdot d^{-1}$): B, PMT_{02T} model; C, H_0 model; D, H_c model; E, PMT_{c2T} model; F, PMT_{OUT} model; G, PMT_{OUH} model and H, PMT_{CUH} model

380

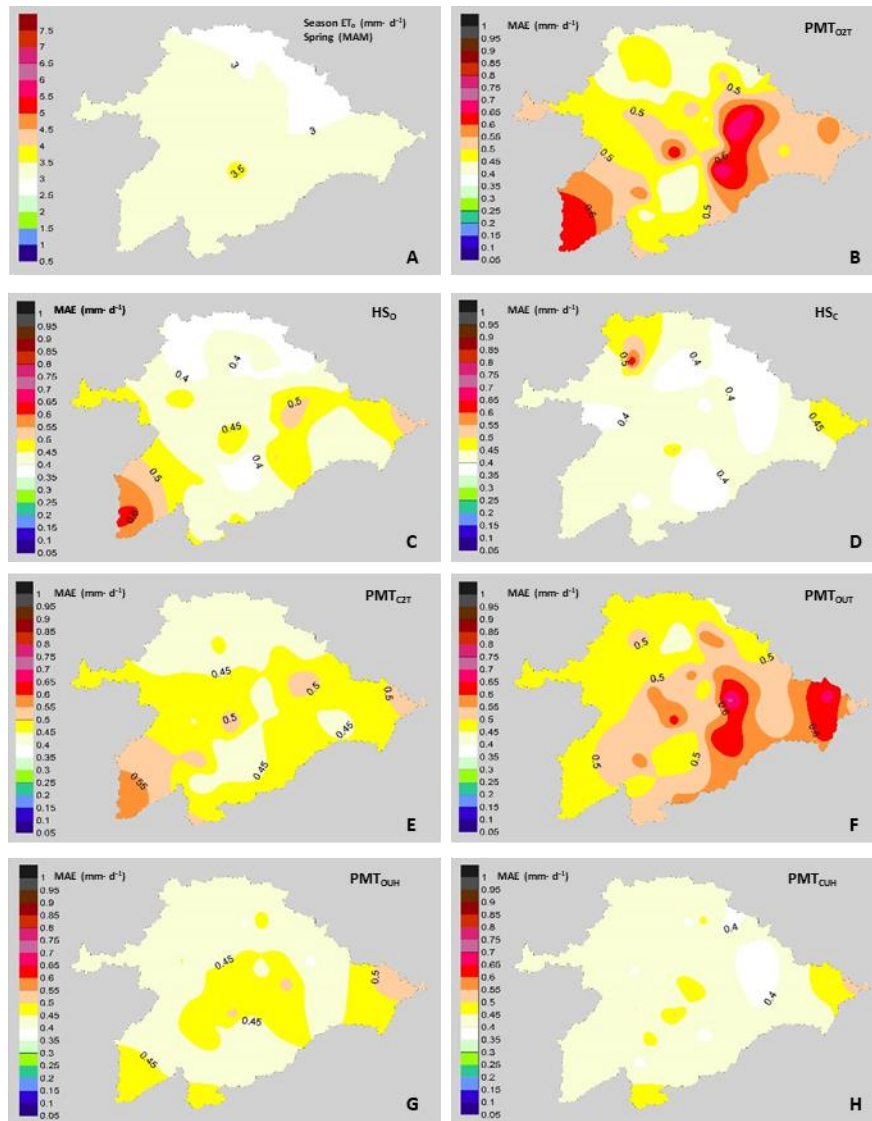
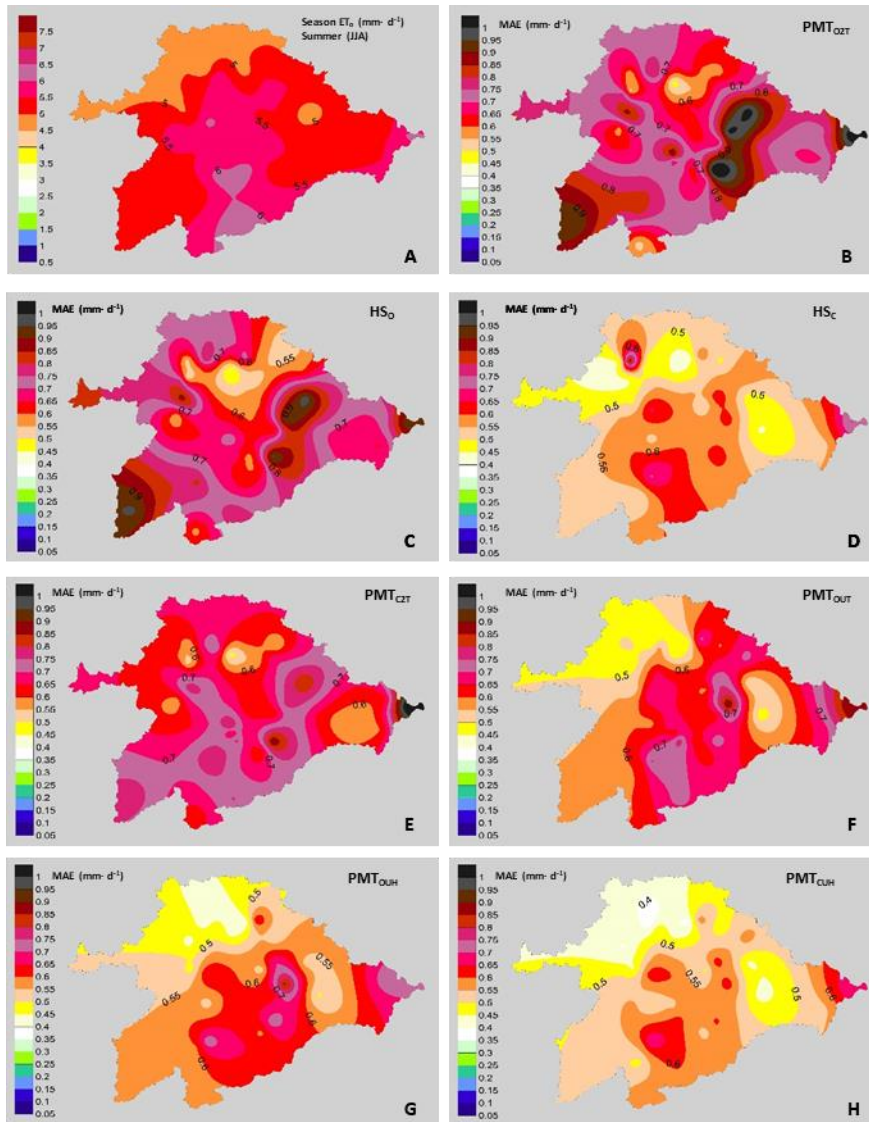


Fig.5. Performance of the models with a spring focus (March, April and May). A, Average annual values of ET_0 ($mm \cdot d^{-1}$) in spring. Mean values of MAE ($mm \cdot d^{-1}$): B, PMT_{O2T} model; C, H_o model; D, H_c model; E, PMT_{C2T} model; F, PMT_{OUT} model; G, PMT_{OUH} model and H, PMT_{CUH} model

390 The model that shows the best performance independently of the seasonal is the PMT_{CUH} . The models that can be considered in a second level are the H_{SC} and the PMT_{OUH} . During the months of more solar radiation (summer and spring) the performance of the H_{SC} model is slightly better than the PMT_{OUH} model. The following models: H_{So} , $PMTO2T$, $PMTC2T$ and $PMTOUT$, have a much lower performance than the previous models (PMT_{OUH} and H_{SC}). The model that has the worst performance is the PMT_{O2T} .

395 The northern area of the basin is the area in which lower MAE shows in most models and for all seasons. This is due in part to the fact that the lower values of ET_0 ($mm \cdot d^{-1}$) are located in the northern zone. On the other hand, the eastern zone of the basin shows the highest values of MAE error due to the strong winds that are located in that area.

During the winter the seven models tested show no great differences between them, although the PMT_{CUH} is the model with the best performance. It is important to indicate that during this season the RMSE (%) is placed in all the models above 30%, so they can be considered as very weak models. According to Jamieson et al. (1991) and Bannayan and Hoogenboom (2009) the model is considered excellent with a normalized RMSE (%) less than 10%, good if the normalized RMSE (%) is greater than 10 and less than 20%, fair if the normalized RMSE (%) is greater than 20% and less than 30%, and poor if the normalized RMSE (%) is greater than 30%. All models that are made during the spring season (MAM) can be considered as good / fair since their RMSE (%) fluctuates between 17-20%. The seven models that are made during summer season (JJA) can be considered as good since their RMSE varies from 12 to 16%. Finally, the models that are made during autumn (SON) are considered fair / poor fluctuating between the values of 22-32%. The models that reached values greater than 30% during autumn were the model PMT_{C2T} (31%) and PMT_{O2T} (32%) also with a clear tendency to overestimation (Table 3) In the use of temperature models for estimating ET_o , it is necessary to know the objective that is set. For the management of irrigation in crops is better to test the models in the period in which the species require the contribution of additional water. In many cases applying the models with an annual perspective with a good performance can lead to more accentuated errors in the period of greater water needs. The studies of different temporal and spatial scales of the temperature models for ET_o estimation, can give valuable information that allow to manage the water planning in zones where the economic development does not allow the implementation of agrometeorological stations due to its high cost.



420 Fig.6. Performance of the models with a summer focus (June, July and August). A, Average values of ET_0 ($mm \cdot d^{-1}$) in summer. Mean values of MAE ($mm \cdot d^{-1}$): B, PMT_{O2T} model; C, H_O model; D, H_C model; E, PMT_{C2T} model; F, PMT_{OUT} model; G, PMT_{OUH} model and H, PMT_{CUH} model

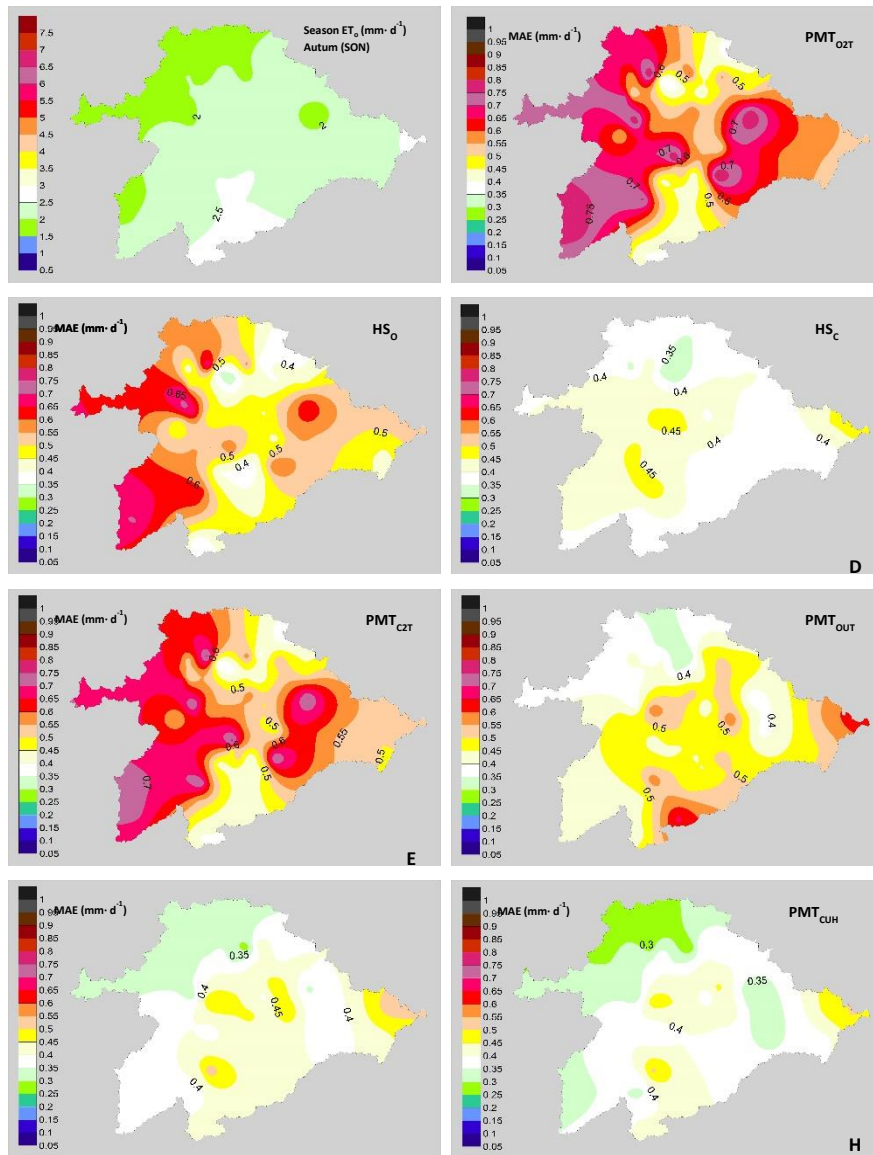


Fig.7. Performance of the models with an autumn focus (September, October and November). A, Average values of ET_0 ($mm \cdot d^{-1}$) in autumn. Mean values of MAE ($mm \cdot d^{-1}$): B, PMT_{O2T} model; C, HS_O model; D, HS_C model; E, PMT_{C2T} model; F, PMT_{OUT} model; G, PMT_{OUH} model and H, PMT_{CUH} model.

4. Discussion

In annual seasons our data of RMSE fluctuates from $0.69 \text{ mm} \cdot d^{-1}$ (PMT_{O2T}) to $0.52 \text{ mm} \cdot d^{-1}$ (PMT_{O2T}). These data are in accordance with the values cited by other authors in the same climatic zone. Jabloun and Sahli (2008) cited RMSE of $0.41\text{-}0.80 \text{ mm} \cdot d^{-1}$ for Tunisia. The authors showed the PMT model performance better than for the Hargreaves non calibrated model. Raziei and Pereira (2013) reported data of RMSE for semiarid zone in Iran between 0.27 and $0.81 \text{ mm} \cdot d^{-1}$ for HS_C model and 0.30 and $0.79 \text{ mm} \cdot d^{-1}$ for PMT_{C2T} , although these authors use monthly averages in their models. Ren et al. (2016) reported values of RMSE in a range of 0.51 to $0.90 \text{ mm} \cdot d^{-1}$ for PMT_{C2T} and range of 0.81 to $0.94 \text{ mm} \cdot d^{-1}$ for HS_C in semiarid locations in Inner Mongolia (China). Todorovic et al. (2013) found that the PMT_{O2T} method have better performance than the uncalibrated HS method (HS_O), with RMSE average of $0.47 \text{ mm} \cdot d^{-1}$ for PMT_{O2T} and 0.52 HS_O . At this point, we should highlight that in our study daily values data have been used.

440 The original Hargreaves equation was developed by regressing cool season grass ET in Davis California,
the k_{RS} coefficient is a calibration coefficient. The Aridity Index for Davis is semiarid ($P/ET=0.33$)
(Hargreaves and Allen, 2003; Moratiel et al. 2013b) like 94% of the stations studied which explains why
the behavior of the HSo model is often very similar to HSc. Even so, the calibration coefficient needs to
be adjusted for other climates. Numerous studies in the literature have demonstrated the relevance of the
445 k_{RS} calibration model for estimating FAO56 (Todorovic et al., 2013, Raziei and Pereira, 2013, Paredes et
al., 2018)

PMT models have improved considering the average wind speed. In addition, trends and fluctuations of u
have been reported as the factor that most influences ET_o trends (Nouri et al., 2017, McVicar et al., 2012;
Moratiel et al., 2011). Numerous authors have recommended to include, as much as possible, average
450 data of local wind speeds for the improvement of the models as Nouri and Homae (2018) and Raziei and
Pereira (2013) in Iran, Paredes et al. (2018) in Azores islands (Portugal), Djaman et al. (2017) in Uganda,
Rojas and Sheffield (2013) in Louisiana (USA), Jabloun and Shali (2008) in Tunisia and Martinez-Cob
and Tejero-Juste (2004) in Spain, among others. In addition, even ET_o prediction models based in PMT
focus their behavior based on the wind speed variable (Yang et al., 2019). It is important to note that the
455 PMT_{OUT} generally has a better performance than the PMT_{C2T} except for spring. The difference between
both models is that in the PMT_{C2T} k_{RS} is calibrated with wind speed set at 2 m/s and in the PMT_{OUT} k_{RS}
is not calibrated and with an average wind. In this case the wind speed variable affects less than the
calibration of k_{RS} since the average values of wind during spring (2.3 m/s) is very close to 2 m/s and there
is no great variation between both settings. In this way, k_{RS} calibration shows a greater contribution than
460 the average of the wind speed to improve the model (Fig.5 E, F). In addition, although u is not directly
considered for HS, this model is more robust in regions with speed averages around 2 m/s (Allen et al.
1998 and Nouri and Homae, 2018) On the other hand errors in the estimation of relative humidity cause
substantial changes in the estimation of ET_o as reported by Nouri and Homae (2018) and Landeras et al.
(2008).

465 The results of RMSE values (%) of the different models change considerably by seasons, values between
16.6% and 12.3% for summer and between 41.2% and 33.5% for winter. Similar results were obtained in
Iran by Nouri and Homae (2018), where the months of December-January and February the performance
of the PMT and HS models tested had RMSE (%) values above 30%. Very few studies, as far as we
470 know, have been carried out of adjustments of evapotranspiration models from a temporal point of view
and generally the models are usually calibrated and adjusted from an annual point of view. Some authors,
such as Aguilar and Polo (2011), differentiate seasons as wet and dry, others such as Paredes et al. (2018)
divide in summer and winter, Vangelis et al. (2013) take into account two periods and Nouri and Homae
(2018) do it from a monthly point of view. In most cases, the results obtained in these studies are not
475 comparable with those performed in this, since the time scales are different. However, it can be indicated
that the results of the models according to the time scale season differ greatly with respect to the annual
scale.

5. Conclusions

480 The performance of seven temperature-based models (PMT and HS) were evaluated in the Duero basin (Spain) with a total of 49 agrometeorological stations. Our studies revealed that the models tested on an annual or seasonal basis provide different performance. The values of R^2 are higher when they are performed annually with values between 0.91-0.93 for the seven models, but when performed from a seasonal perspective there are values that fluctuate between 0.5-0.6 for summer or winter and 0.86-0.81
485 for spring and autumn. The NSE values are high for models tested from an annual view, but for the seasons of spring and summer they are in values below 0.5 for the models HS_o , PMT_{O2T} , PMT_{C2T} and PMT_{OUT} . The fluctuations between models with annual perspective of RMSE and MAE were greater than if those models were compared with a seasonal perspective. During the winter none of the models showed a good performance with values of $R^2 > 0.59$ $NSE > 0.58$ and $RMSE (\%) > 30\%$. From a practical point of
490 view in the management of irrigated crops, winter is a season where crop water needs are minimal with daily average values of ET_o around 1 mm due to low temperatures, radiation and VPD. The model that showed the best performance was PMT_{CUH} followed by PMT_{OUH} and HS_c for annual and seasonal criteria. PMT_{OUH} is slightly less robust than PMT_{CUH} during the maximum radiations periods of spring and summer since the PMT_{CHU} performs the k_{RS} calibration. The performance of the HS_c model is better
495 in the spring period, which is similar to PMT_{CHU} . The spatial distribution of MAE errors in the basin shows that it is highly dependent on wind speeds, obtaining greater errors in areas with winds greater than 2.8 m/s (east of the basin) and lower than 1.3 m/s (south-southwest of the basin). This information of the tested models in different temporal and spatial scales can be very useful to adopt appropriate measures for an efficient water management under limitation of agrometeorological data and under the recent
500 increments of dry periods in this basin. It is necessary to consider that these studies are carried out on a local scale and in many cases the extrapolation of the results on a global scale is complicated. Future studies should be carried out in this line from a monthly point of view since there may be high variability within the seasons.

6. Acknowledgements

505 Financial support provided by MINECO (Ministerio de Economía y Competitividad) through project PRECISOST (AGL2016-77282-C3-2-R) and project AGRISOST-CM (S2018/BAA-4330) is greatly appreciated.

7. References

- 510 Aguilar, C., and Polo, M.J.: Generating reference evapotranspiration surfaces from the Hargreaves equation at watershed scale. *Hydrol. Earth Syst. Sci.*, 15, 2495–2508. <https://doi.org/10.5194/hess-15-2495-2011>.2011
- 515 Allen, R. G.: Evaluation of procedures for estimating grass reference evapotranspiration using air temperature data only. Report submitted to Water Resources Development and Management Service, Land and Water Development Division, United Nations Food and Agriculture Service, Rome, Italy. 1995

- Allen, R. G.: Assessing integrity of weather data for use in reference evapotranspiration estimation. *J. Irrig. Drain. Eng.*, 122, 97–106, [https://doi.org/10.1061/\(ASCE\)0733-9437\(1996\)122:2\(97\)](https://doi.org/10.1061/(ASCE)0733-9437(1996)122:2(97)), 1996.
- 520 Allen, R.G., Pereira, L. S., Howell, T, A., and Jensen, E.: Evapotranspiration information reporting: I. Factors governing measurement accuracy, *Agr. Water Manage.*, 98, 899-920, <https://doi.org/10.1016/j.agwat.2010.12.015>, 2011.
- Allen, R. G., Pereira, L. S., Raes, D., and Smith, M.: Crops evapotranspiration, Guidelines for computing crop requirements, Irrigations and Drainage Paper 56, FAO, Rome, 300 pp., 1998.
- 525 Almorox, J., Quej, V.H., and Martí, P.: Global performance ranking of temperature-based approaches for evapotranspiration estimation considering Köppen climate classes, *J. Hydrol.*, 528, 514-522. <http://dx.doi.org/10.1016/j.jhydrol.2015.06.057>. 2015.
- Annandale, J., Jovanovic, N., Benade, N., and Allen, R.G.: Software for missing data error analysis of Penman-Monteith reference evapotranspiration. *Irrig. Sci.* 21, 57–67, <https://doi.org/10.1007/s002710100047>, 2002.
- 530 Bannayan, M., Hoogenboom, G.: Using pattern recognition for estimating cultivar coefficients of a crop simulation model, *Field Crop Res.*, 111, 290-302. <https://doi.org/10.1016/j.fcr.2009.01.007>. 2009.
- Ceballos, A., Martínez-Fernández, J., and Luengo-Ugidos, M. A.: Analysis of rainfall trend and dry periods on a pluviometric gradient representative of Mediterranean climate in Duero Basin, Spain, *J. Arid. Environ.*, 58, 215–233, <https://doi.org/10.1016/j.jaridenv.2003.07.002>, 2004.
- 535 Djaman, K., Rudnick, D., Mel, V.C., Mutibwa, D., Diop, L., Sall, M., Kabenge, I., Bodian, A., Tabari, H., Irmak, S.: Evaluation of Valiantzas' simplified forms of the FAO-56 Penman-Monteith reference evapotranspiration model in a humid climate. *J. Irr. Drain. Eng.*, 143, 06017005, [https://doi.org/10.1061/\(ASCE\)IR.1943-4774](https://doi.org/10.1061/(ASCE)IR.1943-4774). 2017.
- 540 Droogers, P., and Allen, R.G.: Estimating reference evapotranspiration under inaccurate data conditions. *Irrig. Drain. Syst.*, 16: 33–45, <https://doi.org/10.1023/A:1015508322413>, 2002.
- CHD, Confederación Hidrográfica del Duero: <http://www.chduero.es>, last access: 28 January 2019.
- Estevez, J., García-Marín, A.P., Morábito, J.A. and Cavagnaro, M.: Quality assurance procedures for validating meteorological input variables of reference evapotranspiration in mendoza province (Argentina), *Agric. Water Manag.*, 172: 96–109. <https://doi.org/10.1016/j.agwat.2016.04.019>
- 545 ,2016. Gavián, P., Lorite, J.I., Tornero and Berengera, J.: Regional calibration of Hargreaves equation for estimating reference ET in a semiarid environment. *Agric. Water Manag.*, 81: 257–281. <https://doi.org/10.1016/j.agwat.2005.05.001>, 2006.
- Hargreaves, G.H.: Simplified coefficients for estimating monthly solar radiation in North America and Europe. Departmental Paper, Dept. of BioI. and Irrig. Engrg., Utah State Univ., Logan, Utah. 1994.
- 550 Hargreaves, G.H., and Samani, Z.A.: Estimating potential evapotranspiration., *J. Irrig. Drain. Div.*, 108(3): 225–230. 1982.
- Hargreaves, G.H., and Samani, Z.A.: Reference crop evapotranspiration from ambient air temperature, *Am. Soc. Agric. Eng. (Microfiche Collect. no. fiche no. 85-2517)*. 1985.
- 555 Hargreaves, G.H., and Allen, R.G.: History and Evaluation of Hargreaves Evapotranspiration Equation, *J. of Irrig. and Drain. Eng.*, 129: 53-63, [https://doi.org/10.1061/\(ASCE\)0733-9437\(2003\)129:1\(53\)](https://doi.org/10.1061/(ASCE)0733-9437(2003)129:1(53)), 2003.
- Jamieson, P.D., Porter, J.R., Wilson, D.R.: A test of the computer simulation model ARCWHEAT1 on

- wheat crops grown in New Zealand. *Field Crop Res.* 27, 337-350. [https://doi.org/10.1016/0378-4290\(91\)90040-3](https://doi.org/10.1016/0378-4290(91)90040-3).1991.
- 560 Jabloun, M. D., and A. Sahli.: Evaluation of FAO-56 methodology for estimating reference evapotranspiration using limited climatic data: Application to Tunisia, *Agric. Water Manage.*, 95, 707–715. <https://doi.org/10.1016/j.agwat.2008.01.009>, 2008.
- Landeras, G., Ortiz-Barredo, A., and López, J.J.: Comparison of artificial neural network models and empirical and semi-empirical equations for daily reference evapotranspiration estimation in the Basque Country (Northern Spain). *Agric. Water Manage.* 95: 553–565. <https://doi.org/10.1016/j.agwat.2007.12.011>. 2008.
- 565 Lautensach, H.: *Geografía de España y Portugal*, Vicens Vivens, Barcelona, 814 pp., 1967 (in Spanish).
- López-Moreno, J.I., Hess, T.M., and White, A.S.M.: Estimation of Reference Evapotranspiration in a Mountainous Mediterranean Site Using the Penman-Monteith Equation With Limited Meteorological Data. *Pirineos JACA*, 164, 7–31, <https://doi.org/10.3989/pirineos.2009.v164.27.2009>.
- 570 MAPAMA, Ministerio de Agricultura Pesca y Alimentación, Anuario de estadística. <https://www.mapa.gob.es/es/estadistica/temas/publicaciones/anuario-de-estadistica/>, last access: 28 de March 2019.
- Martinez, C.J., and Thepadia, M.: Estimating Reference Evapotranspiration with Minimum Data in Florida, *J. Irrig. Drain. En.*, 136,494-501, [https://doi.org/10.1061/\(ASCE\)IR.1943-4774.0000214](https://doi.org/10.1061/(ASCE)IR.1943-4774.0000214), 2010.
- 575 Martínez-Cob, A., and Tejero-Juste, M.: A wind-based qualitative calibration of the Hargreaves ET_o estimation equation in semiarid regions, *Agric. Water Manage.* 64(3): 251–264. [https://doi.org/10.1016/S0378-3774\(03\)00199-9](https://doi.org/10.1016/S0378-3774(03)00199-9). 2004.
- McVicar, T.R., Roderick, M. L., Donohue, R.J., Li L.T., G.VanNiel, T., Thomas, A.,Grieser, J., Jhajharia, D., Himri, Y., Mahowald, N.M.,Mescherskaya, A.V., Kruger, A.C., Rehman, S., and Dinpashoh, Y.: Global review and synthesis of trends in observed terrestrial near-surface wind speeds: implications for evaporation. *J. Hydrol.* 416–417: 182–205. <https://doi.org/10.1016/j.jhydrol.2011.10.024>. 2012.
- 580 Mendicino, G., and Senatore, A.: Regionalization of the Hargreaves Coefficient for the Assessment of Distributed Reference Evapotranspiration in Southern Italy, *J. Irrig. Drain. Eng.* 139, 349–62, DOI: 10.1061/(ASCE)IR.1943-4774.0000547, 2012.
- Moratiel, R., Duran, J. M., and Snyder, R.: Responses of reference evapotranspiration to changes in atmospheric humidity and air temperature in Spain, *Clim. Res.*, 44, 27–40, <https://doi.org/10.3354/cr00919>. 2010.
- 590 Moratiel, R., Snyder, R.L., Durán, J.M. and Tarquis, A.M.: Trends in climatic variables and future reference evapotranspiration in Duero valley (Spain). *Nat. Hazards Earth Syst. Sci.* 11, 1795–1805. 2011. <https://doi.org/10.5194/nhess-11-1795-2011>, 2011.
- Moratiel, R., Martínez-Cob, A., and Latorre, B.: Variation in the estimations of ET_o and crop water use due to the sensor accuracy of the meteorological variables. *Nat. Hazards Earth Syst. Sci.*, 13, 1401-1410, <https://doi.org/10.5194/nhess-13-1401-2013>, 2013a.
- 595

Moratiel R., Spano, D., Nicolosi, P. and Snyder, R.L. Correcting soil water balance calculations for dew, fog, and light rainfall. *Irrig Sci* 31:423–429. DOI 10.1007/s00271-011-0320-2, 2013b.

Moriassi, D. N., Arnold, J. G., Van Liew, M. W., Bingner, R. L., Harmel, R. D., and Veith T. L.: Model evaluation guidelines for systematic quantification of accuracy in watershed simulations, *T. ASABE*, 50, 885-900. doi: 10.13031/2013.23153. 2007.

Nash, J. E., and Sutcliffe, J. V: River flow forecasting through conceptual models. Part I—A discussion of principles, *J. Hydrol.* 10, 282–290, [https://doi.org/10.1016/0022-1694\(70\)90255-6](https://doi.org/10.1016/0022-1694(70)90255-6), 1970.

Nouri, M., Homaeae, M., and Bannayan, M.: Quantitative trend, sensitivity and contribution analyses of reference evapotranspiration in some arid environments under climate change. *Water Resour. Manage.* 31 (7), 2207–2224. <https://doi.org/10.1007/s11269-017-1638-1>. 2017.

Nouri, M., and Homaeae, M.: On modeling reference crop evapotranspiration under lack of reliable data over Iran. *J. Hydrol.* 566, 705-718. <https://doi.org/10.1016/j.jhydrol.2018.09.037>. 2018

Pandey, V., Pandey, P.K., and Mahata, P.: Calibration and performance verification of Hargreaves Samani equation in a Humid region. *Irrig. Drain.* 63:659-667. <https://doi.org/10.1002/ird.1874>. 2014

Pandey, P.K., Pandey, V.: Evaluation of temperature-based Penman-Monteith (TPM) model under the humid environment. *Model. Earth Syst. Environ.* 2:152. <https://doi.org/10.1007/s40808-016-0204-9>. 2016.

Paredes, P., Fontes, J.C., Azevedo, E.B., and Pereira, L.S.: Daily reference crop evapotranspiration with reduced data sets in the humid environments of Azores islands using estimates of actual vapor pressure, solar radiation, and wind speed.. *Theor. Appl. Climatol.* 134:1115–1133 <https://doi.org/10.1007/s00704-017-2329-9>. 2018.

Pereira, L.S.: Water, Agriculture and Food: Challenges and Issues, *Water Resour. Manage.*, 31, 2985-2999. <https://doi.org/10.1007/s11269-017-1664-z>, 2017.

Pereira, L.S, Allen, R.G., Smith, M., and Raes, D.: Crop evapotranspiration estimation with FAO56: Past and future, *Agr. Water Manage.*, 147, 4-20, <http://dx.doi.org/10.1016/j.agwat.2014.07.031>, 2015.

Plan Hidrológico, Plan Hidrológico de la parte española de la demarcación hidrográfica del Duero. 2015-2021. Anejo 5. Demandas de Agua. <http://www.chduero.es/Inicio/Planificaci%C3%B3n/Planhidrol%C3%B3gico20162021Vigente/PlanHidro1%C3%B3gico/tabid/734/Default.aspx>. last access: 18 February 2019.

Quej, V.H., Almorox, J., Arnaldo, A., and Moratiel, R.; Evaluation of Temperature-Based Methods for the Estimation of Reference Evapotranspiration in the Yucatán Peninsula, Mexico, *J. Hydrol. Eng.*, 24(2): 05018029, [https://doi.org/10.1061/\(ASCE\)HE.1943-5584.0001747](https://doi.org/10.1061/(ASCE)HE.1943-5584.0001747), 2019.

Raziei, T., and Pereira, L.S.: Estimation of ETo with Hargreaves-Samani and FAO-PM temperature methods for a wide range of climates in Iran, *Agric. Water Manag.* 121, 1–18, <https://doi.org/10.1016/j.agwat.2012.12.019>, 2013.

Rojas, J.P., and Sheffield, R.E.: Evaluation of daily reference evapotranspiration methods as compared with the ASCE-EWRI Penman-Monteith equation using limited weather data in Northeast Louisiana. *J. Irr. Drain. Eng.*, 139, 285–292. [https://doi.org/10.1061/\(ASCE\)IR.1943-4774.0000523](https://doi.org/10.1061/(ASCE)IR.1943-4774.0000523). 2013.

- Ren, X., Qu, Z., Martins, D.S., Paredes, P., and Pereira, L.S.: Daily Reference Evapotranspiration for Hyper-Arid to Moist Sub-Humid Climates in Inner Mongolia, China: I. Assessing Temperature Methods and Spatial Variability, *Water Resour. Manag.*, 30(11), 3769–3791, <http://link.springer.com/10.1007/s11269-016-1384-9>, 2015.
- 640 SIAR, Sistema de información Agroclimática para el Regadío, <http://eportal.mapama.gob.es/websiar/Inicio.aspx>, last access 2 June 2018.
- Segovia-Cardozo, D.A., Rodríguez-Sinobas, L., and Zobelzu, S.: Water use efficiency of corn among the irrigation districts across the Duero river basin (Spain): Estimation of local crop coefficients by satellite images, *Agric. Water Mang.* 212, 241-251, <https://doi.org/10.1016/j.agwat.2018.08.042>, 2019.
- 645 Todorovic, M., Karic, B., and Pereira, L.S.: Reference Evapotranspiration estimate with limited weather data across a range of Mediterranean climates, *J. Hydrol.* 481, 166-176. <http://dx.doi.org/10.1016/j.jhydrol.2012.12.034>, 2013.
- Tomas-Burguera, M., Vicente-Serrano, S.M., Grimalt, M., and Beguería, S.: Accuracy of reference evapotranspiration (ET_o) estimates under data scarcity scenarios in the Iberian Peninsula, *Agr. Water*
- 650 *Manage.* 182, 103–116 <http://dx.doi.org/10.1016/j.agwat.2016.12.013>, 2017.
- Trajkovic, S.: Temperature-based approaches for estimating reference evapotranspiration, *J. Irrig. Drain. Eng.* 131(4), 316-323. DOI: 10.1061/~ASCE!0733-9437~2005!131:4~316!, 2005.
- UNEP, World atlas of desertification. 2nd ed. Edited by N. Middleton and D. Thomas. London: Arnold.
- 655 182 pp, 1997.
- Vangelis, H., Tigkas, D., and Tsakiris, G.: The effect of PET method on Reconnaissance Drought Index (RDI) calculation. *J. Arid Environ.*, 88,130-140. <http://dx.doi.org/10.1016/j.jaridenv.2012.07.020>, 2013.
- Villalobos, F.J., Mateos, L., and Fereres, E.; Irrigation Scheduling Using the Water Balance, In: Principles of Agronomy for Sustainable Agriculture, Villalobos, F.J. and Fereres, E, Springer
- 660 International Publishing, Switzerland, 269-279, 2016.
- Yang, Y., Cui, Y., Bai, K., Luo, T., Dai, J., and Wang, W.: Short-term forecasting of daily reference evapotranspiration using the reduced-set Penman-Monteith model and public weather forecast, *Agr. Water Manage.*, 211,70-80. <https://doi.org/10.1016/j.agwat.2018.09.036>. 2019